All-fiber laser seeded femtosecond Yb:KGW solid state regenerative amplifier

Renchong Lv(吕仁冲), Hao Teng(滕浩), Jiajun Song(宋贾俊), Renzhu Kang(康仁铸), Jiangfeng Zhu(朱江峰), and Zhiyi Wei(魏志义)

What follows is a list of articles you may be interested in

Chirp-dependent ionization of hydrogen atoms in the presence of super-intense laser pulses

Fengzheng Zhu(朱风筝), Xiaoyu Liu(刘晓煜), Yue Guo(郭月), Ningyue Wang(王宁月), Liguang Jiao(焦利光), and Aihua Liu(刘爱华)

Zinc-oxide/PDMS-clad tapered fiber saturable absorber for passively mode-locked erbium-doped fiber laser

F D Muhammad, S A S Husin, E K Ng, K Y Lau, C A C Abdullah, and M A Mahdi

Cascaded optical frequency transfer over 500-km fiber link using regenerative amplifier

Xue Deng(邓雪), Dong-Dong Jiao(焦东东), Jie Liu(刘杰), Qi Zang(臧琦), Xiang Zhang(张翔), Dan Wang(王丹), Jing Gao(高静), Rui-Fang Dong(董瑞芳), Tao Liu(刘涛), Shou-Gang Zhang(张首刚)

Generation of femtosecond laser pulses at 263 nm by $K_3B_6O_{10}Cl$ crystal

Ning-Hua Zhang(张宁华), Shao-Bo Fang(方少波), Peng He(何鹏), Hang-Dong Huang(黄杭东), Jiang-Feng Zhu(朱江峰), Wen-Long Tian(田文龙), Hong-Ping Wu(吴红萍), Shi-Lie Pan(潘世烈), Hao Teng(滕浩), Zhi-Yi Wei(魏志义)

Laser diode end-pumped $Nd:YVO_4$ regenerative amplifier for picosecond pulses

Zhang Zi-Long, Liu Qiang, Yan Ping, Xia Paketi, Gong Ma-Li

All-fiber laser seeded femtosecond Yb:KGW solid state regenerative amplifier[*]

Renchong Lv(吕仁冲)[1,2], Hao Teng(滕浩)[2,3,4,†], Jiajun Song(宋贾俊)[2,3],
Renzhu Kang(康仁铸)[1,2], Jiangfeng Zhu(朱江峰)[1,‡], and Zhiyi Wei(魏志义)[2,3,4,§]

[1] School of Physics and Optoelectronic Engineering, Xidian University, Xi'an 710071, China
[2] Beijing National Laboratory for Condensed Matter Physics, Institute of Physics, Chinese Academy of Sciences, Beijing 100190, China
[3] School of Physical Sciences, University of Chinese Academy of Sciences, Beijing 100049, China
[4] Songshan Lake Materials Laboratory, Dongguan 523808, China

A high efficiency compact Yb:KGW regenerative amplifier using an all-fiber laser seed source was comprehensively studied. With thermal lensing effect compensated by the cavity design, the compressed pulses with energy of 1 mJ at 1 kHz and 0.4 mJ at 10 kHz in sub-400-fs pulse duration using chirped fiber Bragg grating (CFBG) stretcher were demonstrated. A modified Frantz–Nodvik equation was developed to emulate the dynamic behavior of the regenerative amplifier. The simulation results were in good agreement with the experiment. Numerical simulations and experimental results show that the scheme can be scalable to higher energy of multi-mJ, sub-300 fs pulses.

1. Introduction

Laser diode pumped Yb-doped femtosecond lasers with high energy and high power have been received significant attention in many advanced applications, such as laser material micro-processing,[1] generation of terahertz radiation,[2] and attosecond science.[3] Among the ultrafast lasers based on Yb doped gain materials,[4] the femtosecond fiber laser has unique advantages, such as high output power with excellent beam quality, reliability, compactness, and maintenance-free operation. However, the output pulse energy from a single fiber amplifier is limited by the nonlinearity, and the typical maximum output pulse energy is only about 0.1 mJ.[5,6] Currently, there are many reports of high energy output from fiber laser system based on coherent beam combination of many fiber amplifiers,[7,8] the pulse energy is now scalable to 23 mJ at 25 kHz based on the spatiotemporal coherent combination of pulse replicas from 12 parallel large-pitch fiber amplifiers.[9] However, in such a system the requirement of sophisticated technology and lager footprint presents a major hurdle for the compact design.

On the contrary, the femtosecond laser based on bulk gain material is intrinsically suited for high energy amplification, the pulse energy of 54 J has already been demonstrated.[10] Therefore, a hybrid Yb-doped amplifier with solid-state amplifier and fiber frontend raises the intriguing possibility of combining these advantages. In practice, chirped fiber Bragg grating (CFBG) is usually used as a pulse stretcher in the fiber frontend due to its compactness, simplicity of alignment, and robustness. With this hybrid scheme, compact and robust ultrashort pulses have been obtained in Yb:YAG crystal rod power amplifier[11,12] and thin-disk regenerative amplifier (RA) with all-fiber frontend.[13] However, limited by the gain bandwidth, the output pulse duration is around 1 ps.

Achieving shorter pulse often requires a broad gain bandwidth. Among the various Yb-doped bulk gain material, Yb:KGW/KYW is regarded as an ideal gain medium due to the broad gain bandwidth exceeding 18 nm (full-width at half-maximum, FWHM), which corresponds to the Fourier transform limited (FTL) pulse duration of less than 100 fs. For example, a chirped-pulse RA based on Yb:KYW crystal with output energy of 6.3 mJ and pulse duration of 650 fs was developed.[14] And a pulse energy up to 27 mJ at 100 Hz was realized with a pulse duration of 560 fs.[15] Based on the dual-crystal configuration, much shorter pulses of 190 fs[16] and 182 fs pulse durations were achieved at high repetition rate.[17] Recently, the output pulses with energy of 1.2 mJ and pulse duration of 228 fs were demonstrated using dual Yb:KGW crystal configuration in RA at a repetition rate of 1 kHz.[18] Most of the reported research results so far were based on the bulk oscillator and classical Martinez/Öffner stretcher concepts, the short pulse was obtained at the expense of complexity. Al-

though a hybrid Yb:KGW regenerative amplifier was demonstrated, the pulse energy was only 21 μJ at a 60 kHz repetition rate.[19]

In this paper, we theoretically and experimentally investigate the hybrid femtosecond RA based on Yb:KGW. The compact configuration has been achieved with a CFBG stretcher. Counteracting the thermal lensing effect with cavity design, 1 mJ pulses with a pulse duration of 393 fs at 1 kHz repetition rate are obtained. The maximum output power is 4 W at 10 kHz repetition rate. A modified Frantz–Nodvik equation is also developed to analyze the evolutionary dynamics of the amplified pulse and spectra. The theoretical simulation results agree well with the experimental results and show the possibility of scaling up to a higher energy pulse with a pulse duration of less than 300 fs at a higher repetition rate.

2. System design

The experimental setup of the RA is shown in Fig. 1. The all-fiber seed source consists of a home-made all-normal dispersion (ANDi) management femtosecond fiber oscillator, a CFBG stretcher, and a single-mode fiber pre-amplifier. The specially designed CFBG introduces group-delay dispersion (GDD) of 20.24 ps^2, and third-order dispersion (TOD) of 0.146 ps^3 with center wavelength of 1030 nm and operation bandwidth > 20 nm. The pulses from the fiber oscillator are stretched to 600 ps duration using the CFBG stretcher. Subsequently, a single-mode fiber pre-amplifier is adopted to increase the power up to 140 mW. The all-fiber front end of the system employs polarization-maintaining components. The scheme of RA is a linear cavity consisting of two concave mirrors and two flat end mirrors. The thin-film plate (TFP), half wave plate (HWP), and Faraday rotator (FR) are employed to avoid destructive back reflection and separate the amplified pulses from the seeder. A DKDP Pockels cell (PC) with a clear aperture of 8 mm and length of 24 mm is used for pulse injection and ejection. The gain medium in RA is a 5 mm long Yb:KGW (3 at.%) crystal, which is Ng-cut to provide E//Nm and E//Np polarized laser emission. The amplified pulses are finally compressed by a pair of 1600 lines/mm transmission gratings arranged in Littrow configuration.
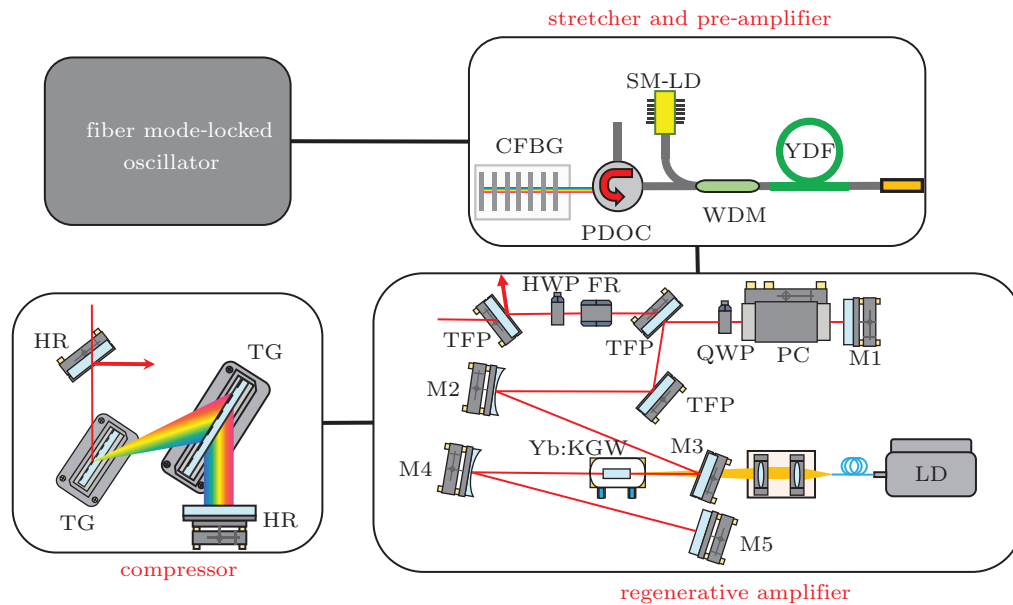

Fig. 1. Schematic of the hybrid amplification system. PDOC: polarization-dependent optical circulator, YDF: Yb-doped fiber, SM-LD: single mode laser diode, WDM: wavelength division multiplex, HWP: half-wave plate, FR: Faraday rotator, QWP: quarter-wave plate, TFP: thin film polarizer, TG: transmission grating, PC: Pockels cell.

2.1. Thermal lensing compensation

The quality of the beam is impaired by the thermal lens. The thermal lens dioptric power can be expressed as[20]

$$D_{th} = \frac{\eta_h P_{abs} \chi}{2\pi \omega_p^2 K_C},\tag{1}$$

where χ is a polarization-averaged thermo-optic coefficient, K_C the thermal conductivity in W·m^{-1}·K^{-1}, P_{abs} is the absorbed pump power, η_h is the fractional thermal load, and ω_p is the beam radius. In practice, the thermal lens with less than 200 mm focal length is induced in Yb:KGW in the case of water-cooling when pumped by more than 30 W pump power.[21] Cavity stability against thermal lens is crucial to the successful operation of the amplifier, as for standard single-crystal RA, placement of the laser crystal slightly off the beam waist in the cavity will resist the deleterious effects of the thermal lensing effect.[22] Taking into consideration of the thermal lensing effect, the resonator mode with a thermal lens of 200 mm is calculated using ABCD matrix formalism, as presented in Fig. 2. The beam diameter along with the Yb:KGW is 0.28 mm.

To better characterize dynamical stability, the beam waist

size in the laser crystal with different thermal focal length is compared. The results of different locations are demonstrated in Fig. 3(a). The positive sign for distance indicates movement towards concave mirror M4. The more sensitive the cavity is to the thermal lens, the faster the output power will be saturated. This phenomenon was observed during the experiment. With 11 mm offset, as shown in Fig. 3, the cavity is stable upon varying thermal lens, the beam radius variation is below 10% with increasing thermal focal lens, thus the thermal lens effect is mitigated to some degree.
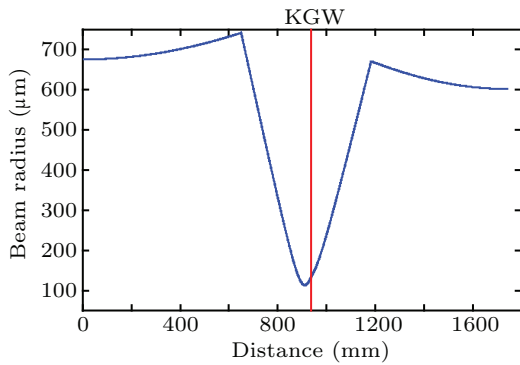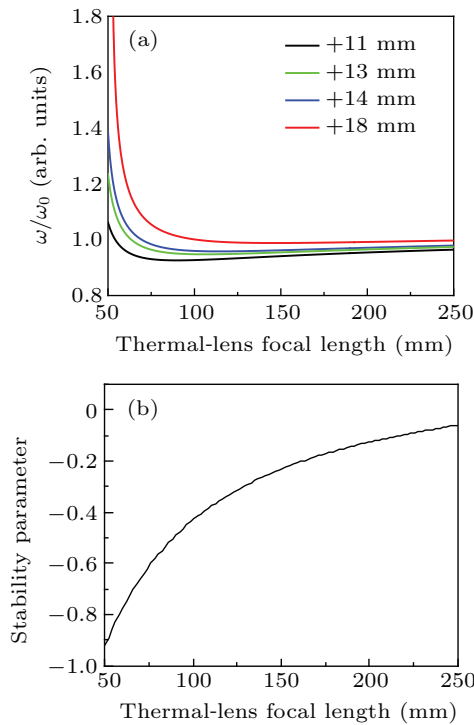

Fig. 2. Calculated beam waist caustic.

Fig. 3. (a) Laser beam radius variation with changed thermal focal length at different displacements. ω and ω_0 are the beam radii at the gain medium with and without thermal lens. (b) Cavity stability (defined as $(A+D)/2$) versus thermal lens.

In order to reduce the heat load, quasi-continuous wave (QCW) pump mode can be employed at a repetition rate of 1 kHz. Approximately 0.4 ms (40% duty cycle) pumping time is chosen, which corresponds to 1.1 times of the Yb:KGW upper state lifetime. This greatly alleviates the thermal effect in the crystal. Moreover, to achieve good heat transfer from the crystal, the crystal rod is wrapped with an indium foil, and soldered with copper heat sink by heating in a vacuum furnace. The soldering process effectively increases the thermal conductivity at the interface and ensures the efficient cooling of the crystal.

2.2. Simulation model

Due to the low net gain of the Yb:KGW crystal, the pulse typically circulates several tens of roundtrips in the regenerative cavity. Therefore, a comprehensive understanding of the dynamics for RAs can provide insight into bifurcation control and gain narrowing compensation.[23] Numerical simulation is carried out based on a modified Frantz–Nodvik equation.[24,25] The incoming pulse fluence is partitioned in time slices Δt, and the gain medium of length L is split into smaller propagation slices Δz. The inversion fraction, defined as $\beta = n_e / N_{\text{total}}$, with n_e representing the number of excited ions and N_{total} the total number of ions in the considered gain volume, is updated in each slice with iteration. Calculating the spectral gain and fluence, the model can provide faster approaches with accurate reproducibility of energy and spectra. With a pump power of 45 W and seed energy of 1 nJ with spectral bandwidth covering from 1020 nm to 1050 nm, the simulation results show that the pulse energy is amplified to 2 mJ when the seed laser is circulated in the regenerative cavity for 35 rounds at 1 kHz repetition rate. Figure 4(a) shows the energy building process and the single-pass gain. The gain has reached saturation after 35 roundtrips and the output energy will drop as the number of amplifications continues to increase. The evolution of output spectrum along the amplification process is also depicted in Fig. 4(b), the pulse spectral bandwidth gradually reduces due to gain narrowing.
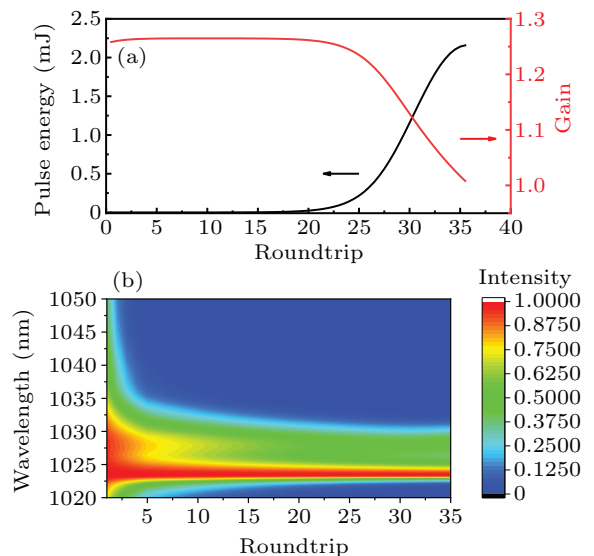

Fig. 4. Simulated evolution of the pulse energy, gain (a) and spectrum (b) during amplification.

3. Results and discussion

The home-made all-fiber oscillator, which is typical mode-locked by nonlinear polarization evolution (NPE), produces 4.7 ps pulse at 1030 nm with 40.3 MHz repetition rate and 50 mW average power. The seed pulses have 20 nm spectral bandwidth, which corresponds to FTL pulse duration of 85 fs.

The seed pulses stretched by CFBG are amplified to 3 nJ with a single-mode fiber amplifier. The pulses are then injected into the regenerative cavity. By optimizing orientation of the PC and delay between the seed and pump, the amplified pulse with a maximum energy of 1.5 mJ is extracted from the regenerative cavity at a 1 kHz repetition rate. The optimized timing corresponds to 35 round trips in the regenerative cavity. Considering the loss in the optical path, the injected pulse energy was 1 nJ, thus the overall amplification of RA is 1.5×10^6, and the amplification per pass is 1.225.
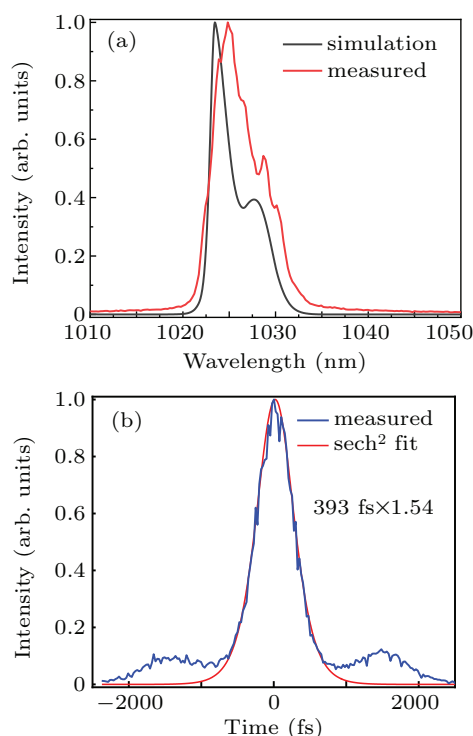

Fig. 5. (a) Measured (red) and simulated (black) spectra of the amplifier. (b) AC traces of pulses from the regenerative amplifier (blue) and sech^2-fit (red).

During amplification, the polarization of pulses is set to parallel to the Nm axis, and the shorter wavelength in pulses gains more due to the gain maxima centered at 1025 nm. The evolution of the spectrum is evaluated. Figure 5(a) presents the measured and simulated output spectra from the regenerative amplifier. The simulated results are generally in good agreement with the experiment, but there are intensity differences in some spectral ranges due to the lack of accurate absorption and emission cross-sections and the fact that the wavelength-dependent losses in the cavity have not been accurately measured. Such spectral bandwidth can support a 280 fs

FTL pulse. With the optimization of the dispersion compensation, as shown in Fig. 5(b), the shortest pulse with a duration of 393 fs is obtained, while the pulse energy from the compressor is 1 mJ, corresponding to a 67% compression efficiency. The discrepancy between the compressed pulse and the FTL pulse is attributable to the residual high order dispersion.

Table 1. Pulse energy and average power of the RA with different repetition rates.

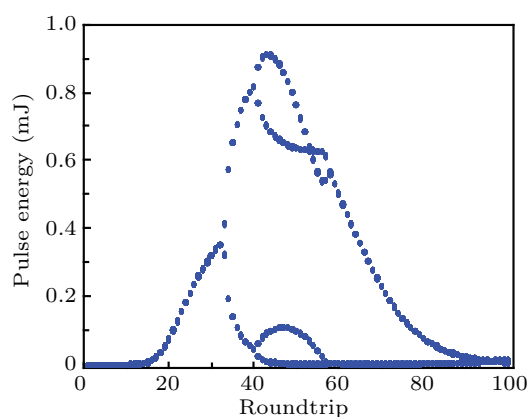| Repetition rate (kHz)	Uncompressed pulse energy (mJ)	Uncompressed average power (W)
1	1.5	1.5
3	1.22	3.66
5	1.1	5.5
8 (period doubling)	0.8	3.2
10	0.56	5.6

Fig. 6. Simulated bifurcation diagram for different roundtrip at a repetition rate of 8 kHz.

The amplifier can also operate at higher repetition rates (> 3 kHz) with continuous wave (CW)-pumping. Table 1 depicts the pulse energy and average power at different repetition rates. As the repetition rate is increased, the amplified pulse energy is decreased to ~ 500 μJ at 10 kHz repetition rate even though there is more roundtrip. This is due to the fact that the available gain is lower while the repetition rates exceed the frequency corresponding to the spontaneous emission lifetime of the Yb:KGW. Remarkably, when the PC is driven at an 8 kHz repetition rate, the bifurcation phenomena are observed. A period-doubling bifurcation appears, which results in amplified pulses with a repetition rate of 4 kHz. The simulation results give insight into the phenomenon, as shown in Fig. 6. Twenty operation cycles have been conducted, in which one operation cycle includes a pumping process and an amplification process. The pulse energies of subsequent pulses have been calculated and plotted as a function of the number of the roundtrip, which corresponds to the transmission gate time of PC in the cavity. For a short gate time, the RA is able to recover the gain and the system is stable. However, with the gate time increasing, the energy of the amplified pulse increases while the gain decreases, the gain cannot recover for the next cycle, the system becomes unstable. In the simulation, as the

roundtrip exceeds 30, period-doubling appears. Although reducing the number of roundtrips in the cavity can avoid bifurcation, the efficiency of amplification is sacrificed, there is a trade-off between output energy and extraction efficiency. Achieving optimal performance often requires carefully chosen pump power, repetition rate, and gate time of PC.

The compact cavity we developed enables a TEM$_{00}$ output at all output power levels, despite the thermal lens change at different repetition rates. The measured M^2 value of the output beam at 1 kHz is 1.24 and 1.32 in the X and Y axis, respectively, as depicted in Fig. 7. Due to the good compensation of the thermal lensing, the cavity works stably and the output beam profile varies little with different repetition rates. The output power is measured to be 1.07 W at 1 kHz repetition rate, and the power stability is 0.4% (RMS) in 2 hours. The stability remains the same with increasing repetition rate.
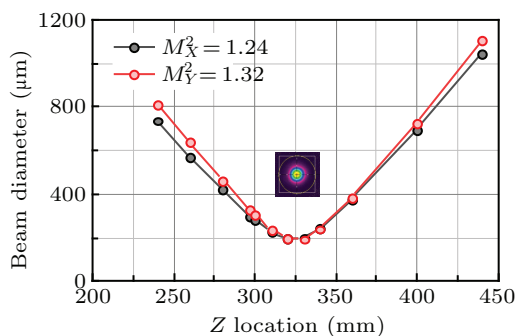

Fig. 7. The M^2 value of output beam from the compact RA system.

For comparison, the RA working along the Np axis is also investigated. As shown in Fig. 8, the amplified pulse has a spectral bandwidth of 5 nm centered at around 1040 nm, but it is at the edge of the spectral distribution of the seed pulse, the phase is nonlinear, the high quality compressed pulse is difficult to obtain.
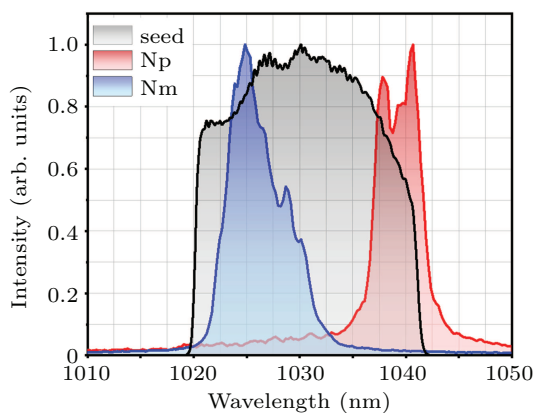

Fig. 8. Spectra of seed (black) and amplified pulses for Nm axis (blue) and Np axis (red).

Based on the above experimental results, in order to obtain a shorter pulse with high energy at high repetition rate between 1–10 kHz, it is necessary to control the gain narrowing

and thermal lensing effect simultaneously. Cryogenic cooling is a good solution to counteract the thermal lensing effect and improve the system performance. At cryogenic temperatures, re-absorption can be suppressed to some extent. Also, the thermo-mechanical properties become more favorable at lower temperatures. Moreover, spectral shaping techniques such as Etalon,[26] Lyot filter,[14] and the AOPDF[27] can be introduced in the RA cavity. Alternatively, dual-crystal configuration exploits the combination of different emission spectra to increase the effective gain bandwidth. To make full use of the gain bandwidth, it is preferable to utilize a broadband seed. For this purpose, parabolic amplification can be employed as a fiber pre-amplifier, as described in Ref. [28]. With this method, pulses with 60 nm bandwidth at 10 dB that supports the generation of sub-60 fs pulse were obtained. We simulate the dynamic of amplification at 10 kHz by introducing spectral profiling, the amplified pulses can possess spectral bandwidth of 10 nm at 10 dB with pulse energy up to 5 mJ, which supports a sub-300 fs pulse. We believe, using the improved solution described above, high fidelity pulses can be achieved with pulse energy of more than 5 mJ and pulse duration of less than 300 fs at repetition rate of 1–10 kHz.

4. Conclusion

We demonstrated an efficient and high energy hybrid Yb:KGW regenerative amplifier with fiber laser frontend at a repetition rate of 1–10 kHz. Taking advantage of thermal lens compensation, the laser system can produce 1 mJ pulse energy at 1 kHz, and 0.4 mJ pulse energy at 10 kHz in less than 400 fs. Moreover, a modified Frantz–Nodvik equation was applied for chromatic simulations in the regenerative amplifier. Further improvements are proposed and discussed, up to 5 mJ of pulse energy in less than 300 fs at repetition rate up to 10 kHz could be scalable with elaborate design. Such compact high energy ultrashort lasers will be attractive for various applications.

References

[1] Bonamis G, Mishchick K, Audouard, E, Hönninger C, Mottay E, Lopez J and Manek-Hönninger I 2019 *Journal of Laser Applications* **31** 022205
[2] Tokita S, Sakabe, S, Nagashima T, Hashida M and Inoue S 2015 *Sci. Rep.* **5** 8268
[3] Lorek E, Larsen E W, Heyl C M, Carlström S, Paleček D, Zigmantas D and Mauritsson J 2014 *Rev. Sci. Instru.* **85** 123106
[4] Saraceno C J, Sutter D, Metzger T and Ahmed M A 2019 *Journal of the European Optical Society-Rapid Publications* **15** 15
[5] Zhao Z G and Kobayashi Y 2015 *Appl. Phys. Express* **9** 012701
[6] Lv Z G, Yang Z, Li Q L, Li F, Wang Y S, Zhao W and Yang X J 2020 *High Power Laser Science and Engineering* **8** 40
[7] Müller M, Kienel M, Klenke A, Gottschall T, Shestaev E, Plötner M, LIMPERT J and Tünnermann A 2016 *Opt. Lett.* **41** 3439
[8] Kienel M, Müller M, Klenke A, Limpert J and Tünnermann A 2016 *Opt. Lett.* **41** 3343

[9] Stark H, Buldt J, Müller M, Klenke A, Tünnermann A and Limpert J 2019 *Opt. Lett.* **44** 5529

[10] Hornung M, Liebetrau H, Keppler S, Kessler A, Hellwing M, Schorcht F, Becker G, Reuter M, Polz J, Körner J, Hein J and Kaluza M 2016 *Opt. Lett.* **41** 5413

[11] Veselis L, Bartulevicius T, Madeikis K, Michailovas A and Rusteika N 2018 *Opt. Express* **26** 31873

[12] Verne L, Petelin J and Petkovšek R 2020 *Opt. Express* **28** 7875

[13] Fischer J, Heinrich A C, Maier S, Jungwirth J, Brida D and Leitenstorfer A 2016 *Opt. Lett.* **41** 246

[14] Calendron A L, Çankaya H and Kärtner F X 2014 *Opt. Express* **22** 24752

[15] Papadopoulos D N, Pellegrina A, Ramirez L P, Georges P and Druon F 2011 *Opt. Lett.* **36** 3816

[16] Buettner A, Buenting U, Wandt D, Neumann J and Kracht D 2010 *Opt. Express* **18** 21973

[17] Kim G H, Yang J H, Lee D S, Kulik A V, Chizhov S A, Kang U and Yashin V E 2013 *Journal of Optical Technology* **80** 142

[18] He H J, Yu J, Zhu W T, Guo X Y, Zhou C T and Ruan S C 2020 *High Power Laser Science and Engineering* **8** 35

[19] Yan D Y, Liu B W, Chu Y X, Song H Y, Chai L, Hu M L and Wang C Y 2019 *Chin. Opt. Lett.* **17** 041404

[20] Chénais S, Druon F, Forget S, Balembois F and Georges P 2006 *Progress in Quantum Electronics* **30** 89

[21] Hoos F, Li S, Meyrath T P, Braun B and Giessen H 2008 *Opt. Express* **16** 6041

[22] Magni V 1987 *JOSA A* **4** 1962

[23] Grishin M, Gulbinas V and Michailovas A 2007 *Opt. Express* **15** 9434

[24] Kroetz P, Ruehl A, Murari K, Çankaya H, Kärtner F X, Hartl I and Miller R D 2016 *Opt. Express* **24** 9905

[25] von Grafenstein L, Bock M and Griebner U 2018 *IEEE Journal of Selected Topics in Quantum Electronics* **24** 1

[26] Ogawa K, Akahane Y, Aoyama M, Tsuji K, Tokita S, Kawanaka J, Nishioka H and Yamakawa K 2007 *Opt. Express* **15** 8598

[27] Golinelli A, Chen X, Gontier E, Bussière B, Tcherbakoff O, Natile M, D'Oliverira P, Paul P M and Hergott J F 2017 *Opt. Lett.* **42** 2326

[28] Lavenu L, Natile M, Guichard F, Zaouter Y, Hanna M, Mottay E and Georges P 2017 *Opt. Express* **25** 7530